Protein Contributions to Redox Potentials of Homologous Rubredoxins: An Energy Minimization Study

Paul D. Swartz and Toshiko Ichiye
Department of Biochemistry and Biophysics, Washington State University, Pullman, Washington 99164-4660 USA

ABSTRACT The energetic contributions of the protein to the redox potential in an iron-sulfur protein are studied via energy minimization, comparing homologous rubredoxins from *Clostridium pasteurianum, Desulfovibrio gigas, Desulfovibrio vulgaris*, and *Pyrococcus furiosus*. The reduction reaction was divided into 1) the change in the redox site charge without allowing the protein to respond and 2) the relaxation of the protein in response to the new charge state, focusing on the latter. The energy minimizations predict structural relaxation near the redox site that agrees well with that in crystal structures of oxidized and reduced *P. furiosus* rubredoxin, but underpredicts it far from the redox site. However, the relaxation energies from the energy-minimized structures agree well with those from the crystal structures, because the polar groups near the redox site are the main determinants and the charged groups are all located at the surface and thus are screened dielectrically. Relaxation energies are necessary for good agreement with experimentally observed differences in reduction energies between *C. pasteurianum* and the other three rubredoxins. Overall, the relaxation energy is large (over 500 mV) from both the energy-minimized and the crystal structures. In addition, the range in the relaxation energy for the different rubredoxins is large (300 mV), because even though the structural perturbations of the polar groups are small, they are very near the redox site. Thus the relaxation energy is an important factor to consider in reduction energetics.

INTRODUCTION

Iron-sulfur proteins are an important class of electron transfer proteins that participate in a wide variety of biological reactions and are found in a wide variety of organisms. The small (M_r 6000 Da) iron-sulfur protein rubredoxin comes primarily from anaerobic bacteria and appears to play a role in electron transport and nitrate reduction (Seki et al., 1989; Hugenholtz and Ljungdahl, 1989). The iron-sulfur site in rubredoxin consists of an iron atom tetrahedrally ligated to four cysteinyl sulfurs, and is the easiest complex to understand in terms of its redox properties.

One important property of an electron transfer protein is its redox potential, because it determines the energetics and rates of electron transfer to its donor and from its acceptor. However, proteins with the same redox site can have different redox potentials (Moura et al., 1979; Lovenberg and Sobel, 1965). In similar 4Fe-4S proteins, the differences in redox potential cannot be attributed to differences in the redox site (Backes et al., 1991), so that they are attributed to the protein environment instead (Sweeney and Rabinowitz, 1980). The work here addresses how different protein environments can influence the redox potential. Rubredoxin is ideal for study, because there are five homologous rubredoxins for which high-resolution (<2.0 Å) crystal structures have been solved (Frey et al., 1987; Watenpaugh et al., 1980; Stenkamp et al., 1990; Adman et al., 1991; Day et al., 1992), four of which have reported redox potentials ranging from +6 to −57 mV (Moura et al., 1979; Adams, 1992; Lovenberg and Sobel, 1965; LeGall et al., 1988). The rubredoxin structures are all highly similar in backbone structure and have ~50–60% sequence identity (Fig. 1).

An earlier study examined the electrostatic potential of crystal structures of these rubredoxins (Swartz et al., 1996). This work identified the determinant of a 50-mV lower redox potential in one of the four rubredoxins as a Val at residue 44 rather than a Ala, which causes a concerted shift in the backbone polar groups, and further confirmed this result by using sequence and redox potential data for nine other rubredoxins. However, this work neglected the contribution of protein relaxation upon reduction to the redox potential, which has been shown to be substantial (up to −16 kcal/mol) for *Clostridium pasteurianum* rubredoxin (Shenoy and Ichiye, 1993). Therefore, the present work examines whether protein relaxation also contributes to the different redox potentials observed in other homologous rubredoxins.

Of the contributions to the reduction energy of a protein, the electrostatic energy is generally the largest of the environmental contributions (i.e., apart from the intrinsic energy difference of the metal site). The electrostatic energy can come from three different sources: charged groups, polar groups, and solvent water. Several experimental results suggest that surface charges (e.g. charged side chains) contribute little to the electrostatic component of redox potential. For instance, experiments on redox proteins in which a charged amino acid residue is mutated to a neutral residue show relatively little effect on the redox potential (Shen et al., 1994; Gleason, 1992). In other experiments, replacement of nonconserved nonpolar residues immediately adja-

Received for publication 3 February 1997 in final form 5 August 1997.

Address reprint requests to Dr. Toshiko Ichiye, Department of Biochemistry and Biophysics, Washington State University, P.O. Box 644660, Pullman, WA 99164-4660. Tel.: 509-335-7600; Fax: 509-335-9688; E-mail: ichiye@wsu.edu.

Dr. Swartz's present address is Department of Biochemistry, Texas A&M University, College Station, TX.

0006-3495/97/11/2733/09 $2.00

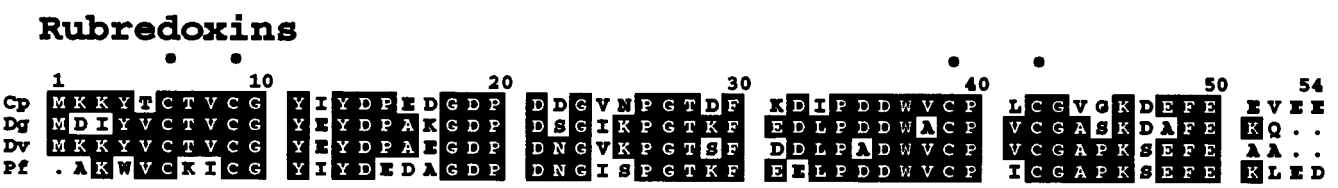

FIGURE 1 Alignment of the sequences for the rubredoxin from *C. pasteurianum* (Cp), *D. gigas* (Dg), *D. vulgaris* (Dv), and *P. furiosus* (Pf). Cysteines ligating the iron are indicated by dots.

cent to the iron-coordinating cysteines in *C. pasteurianum* rubredoxin with either a negative Asp or a positive Arg slightly increases the redox potential (Zeng et al., 1996), indicating that the charged nature of these side chains is unimportant. In addition, Warshel and co-workers have shown good correlation of electrostatic potential with experimental redox potentials in cytochrome *c* (Churg and Warshel, 1986; Langen et al., 1992a) and 4Fe-4S proteins (Langen et al., 1992b), using a model in which the side chains that are normally charged at pH 7.0 are neutralized, although a more recent study of the 4Fe-4S proteins gave poorer results (Jensen et al., 1994). Furthermore, calculations of the electrostatic potential from the crystal structures of four rubredoxins indicate that the solvation energy due to water alone can significantly dampen charged side-chain contributions and that the contributions of the polar backbone and polar side chains correlate with the redox potentials if the charged side chains (which are all at the surface) and solvent contributions are neglected (Swartz et al., 1996). These results are compelling evidence that surface-charged side chains contribute little to the redox potential, leaving the polar side chains and backbone and the solvent accessibility as the only distinguishing features in homologous proteins without buried charged groups such as the rubredoxins. Moreover, in the case of native rubredoxins, solvent accessibility does not appear to be a factor (Swartz et al., 1996).

Given these results, it is reasonable to propose that the reduction energy, including the relaxation energy, due to polar groups in rubredoxins should correlate with the redox potentials. Hence a series of energy minimization studies similar to those on *C. pasteurianum* rubredoxin by Shenoy and Ichiye (1993) were performed on four rubredoxins of known redox potential and well-defined crystal structure to understand the structural and energetic differences leading to the observed differences in redox potential. The reasons for using energy minimizations rather than molecular dynamics simulations, even though the latter will give the important contributions from thermal fluctuations, are as follows. The first reason concerns the potential energy functions used in the calculations. Molecular dynamics simulations will explore more conformations because of the thermal fluctuations, which in theory should lead to a more accurate prediction of structural changes upon change in redox state. However, this is dependent on the accuracy of the potential energy surface. Because errors in the potential energy may lead to a series of structural perturbations that cause the structure to wander further and further from a correct structure, energy minimizations are used here to look for the minimum and thus most likely changes. Thus the gentlest possible minimization procedures for the relaxation step were used, so that the results represent the minimum possible changes. The second reason concerns the electrostatic interactions, which are the controlling interactions for changes in the redox state. Because molecular dynamics simulations are computationally intensive, long-range electrostatic interactions in protein simulations must be handled by approximate methods, such as cutoffs with or without periodic boundary conditions or Ewald sums with periodic boundary conditions (Allen and Tildesley, 1987). Because of possible anomalies due to these methods (see, for instance, Steinbach and Brooks, 1994), the less computationally intensive method of energy minimization was used here, so that no cutoffs in the electrostatics were necessary.

In the Results section, the minimized structures are compared with crystal structures, and the degree of relaxation is compared with that between the crystal structure studies of oxidized and reduced *Pyrococcus furiosus* rubredoxin (Day et al., 1992). Moreover, the contributions of both the change in electrostatic energy of the initial structure upon change in redox site charge (without relaxation) and the relaxation energy to the observed differences in redox potentials of the homologous rubredoxins are studied.

METHODS

The crystal structures of oxidized rubredoxin from *Clostridium pasteurianum* (Cp) at 1.2-Å (Watenpaugh et al., 1980), *Desulfovibrio gigas* (Dg) at 1.4-Å (Frey et al., 1987), and *Desulfovibrio vulgaris* (Dv) at 1.5-Å resolution (Adman et al., 1991) were taken from the Brookhaven Protein Data Bank (PDB). The crystal structures of oxidized and reduced rubredoxin from *Pyrococcus furiosus* (Pf) at 1.8-Å resolution (Day et al., 1992) were provided by Dr. Douglas Rees and are available from the PDB.

Protein relaxation

Energy minimization and energy calculations were performed with the molecular mechanics and dynamics program CHARMM22g3 (Brooks et al., 1983). All energy minimizations were performed with charged side chains,

even though the polar contributions to the energy are focused on. Energy parameters and topologies from CHARMM19 (Brooks et al., 1983) plus additional parameters for the iron-sulfur redox site (Yelle et al., 1995) were used. The nonpolar hydrogens were treated implicitly with the extended atom method, and bonds containing polar hydrogen were constrained to their equilibrium bond length with the SHAKE algorithm (Rychaert et al., 1977). All energy interactions were included in the energy calculations, so that no cutoffs were used. Water molecules were modeled using the TIP3P potential (Jorgensen, 1981). To ensure uniformity among the different rubredoxins, new polar hydrogen positions were generated for each of the rubredoxins even if hydrogen positions were reported in the crystal structures.

The oxidized and reduced forms of rubredoxin are distinguished in the computational model, both in the potential energy function and in the structure. The potential energy parameters for the iron-sulfur site differ for the oxidized and reduced states, not only in the partial charges but also in the equilibrium bond lengths and angles (Yelle et al., 1995). High-resolution crystal structures of both the oxidized and reduced forms of rubredoxin are only available for Pf; therefore the oxidized structure was simulated by energy minimizing the oxidized crystal structure with energy parameters for the oxidized form to obtain a structure referred to as OXD, and the reduced structure was simulated by energy minimizing the minimized oxidized structure with energy parameters for the reduced form to obtain a structure referred to as RED′. In addition, a Frank-Condon state, referred to as RED*, is actually the OXD structure of the protein, but with the energetics calculated using the energy parameters of the reduced form.

Because the object of this work is to compare the energies of the oxidized and reduced states of rubredoxins, it was necessary to perform extensive minimization on the proteins so that convergent structures could be obtained. The procedure used here to obtain the structures in the reaction (Fig. 2) is similar to that used by Shenoy and Ichiye (1993), with a few exceptions. Crystal structures of all four rubredoxins were prepared similarly for energy minimization. First, to relieve high-energy interactions, the newly generated polar hydrogens, including crystal waters and protein hydrogens, were energy minimized while all other atoms were held fixed by unconstrained adopted basis set Newton-Raphson (ABNR) (Brooks et al., 1983) energy minimization with no energy cutoff values. Next, because different crystal structures have different amounts of resolved crystal water, the protein structures were then solvated with additional water molecules, unlike in the method of Shenoy and Ichiye (1993), where only crystal waters were included. This was accomplished by overlapping the protein with a 41-Å cubic box of previously equilibrated water and removing overlapping waters within 2.6 Å and any waters further than 5.0 Å from protein or crystal water atoms, so that all proteins have similar solvation (Shenoy, 1992). The added water molecules were then energy minimized to eliminate any voids and high-energy interactions, using unconstrained ABNR minimization with no energy cutoff values on all waters (including crystal waters) with all protein atoms held fixed. OXD was obtained by unconstrained ABNR energy minimization with no energy cutoff values, of the oxidized crystal plus all waters, with oxidized parameters, until the total energy change over the final 30 steps was less than 0.01 kcal/mol. The RED′ state of rubredoxin was obtained by harmonically constrained ABNR energy minimization (Bruccoleri and Karplus, 1986) with no energy cutoff values of OXD plus all waters, with reduced parameters. The harmonically constrained minimization helps to ensure that the structure does not change much.

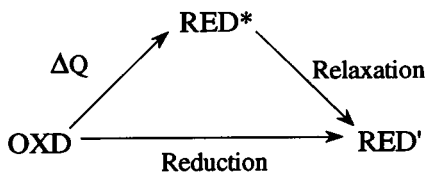

FIGURE 2 Reduction cycle for the energy minimization study. The minimized oxidized protein (OXD) first undergoes an instantaneous charge change (ΔQ) to form the oxidized protein structure with a reduced redox site (RED*), which is followed by a relaxation of the protein structure to accommodate the new charge (Relaxation) for the reduced form of the protein (RED′). The sum of the ΔQ and Relaxation steps is the reduction of the protein (Reduction).

Energy calculations

The relationship between the standard free energy change upon reduction, ΔG, and the redox potential, $E°$, is given by

$$-nF\Delta E° = \Delta G$$

where F is Faraday's constant and n is the number of electrons transferred. In this work, the entropy differences between the four rubredoxin proteins were assumed to be negligible. The change in energy due to the redox reaction may be divided into energy changes due to the charge change, and that due to the relaxation of the protein and solvent in response to the charge change. The energies were total energies for the system calculated in the various states in Fig. 2.

RESULTS

The structural results of the energy minimization studies of the four rubredoxins are presented here, followed by the energetics. The sequence alignment and numbering scheme for the four rubredoxins is given in Fig. 1.

Initial energy minimization

The root mean square deviations (RMSDs) in atomic positions averaged over all N, Cα, and C backbone atoms, between the crystal and energy-minimized protein struc-

tures are presented in Table 1. The RMSDs of the OXD structures from XOXD, the oxidized crystal structures, were all less than 0.9 Å, indicating that the energy minimization method used here is gentle and avoids dramatic structural deformation. In comparing the XOXD to the OXD structure, the rubredoxin from Cp has one significant difference compared to Dg, Dv, and Pf near the redox site. In Cp rubredoxin, energy minimization to the OXD structure causes the amide group of Cys^9, which is ligated to the iron, to move 0.06 Å away from the redox site, whereas in Dg, Dv, and Pf rubredoxins, Cys^9 moved between 0.06 and 0.20 Å closer to the redox site. The backbone amide group of Cys^9 is one of the closest protein polar groups to the redox site (N-Fe distance of 3.8 Å), with the other being the backbone amide group of Cys^{42} in all four rubredoxins.

Structural relaxation upon reduction

The RMSDs upon reduction (Table 1) show that structural changes on reduction of OXD to RED′ are minimal, with average backbone RMSDs of ~0.08 Å, for the four rubredoxins. Most significantly, they are localized around the cysteines that coordinate the redox site (Fig. 3). The RMSDs per residue for backbone atoms alone between the OXD and RED′ structures indicate that structural relaxation is very similar in all of the rubredoxins (Fig. 3). Not only did the largest deviations occur at comparable residues, but the magnitudes of the displacements differ by only ~0.05 Å. The largest displacements in all cases were localized around the cysteine residues that coordinate the iron; for instance, upon reduction of the redox site, the backbone amides of Cys^9 and Cys^{42} moved between 0.10 and 0.23 Å farther from the redox site. In addition, in the first redox site-coordinating loop, the conserved Gly^{10} consistently showed large RMSDs in all of the rubredoxins. However, in the second coordination loop, the semiconserved nonpolar residue 41 showed large relaxation in Dv and Dg rubredoxins, whereas the conserved Gly^{43} showed relaxation in Cp and Pf. Furthermore, in Cp and Pf, the backbone of Glu^{48} showed considerable relaxation, whereas in Dg and Dv, Phe^{49} showed relaxation (Fig. 3).

Because crystal structures of both the oxidized and reduced Pf rubredoxin (Day et al., 1992) have been solved, the structural relaxation predicted by the energy minimization can be compared with experiment. Compared to the average backbone RMSD of 0.24 Å between the oxidized and reduced crystal structures of Pf, the structural deviations of ~0.08 Å in the minimization studies constitute a lower estimate. However, the discrepancies were not the same throughout the protein, as seen in a comparison of the backbone atom RMSD per residue between oxidized and reduced states per residue for the crystal and the minimized structures for Pf rubredoxin (Fig. 3). The largest RMSD for any residue in the minimized structures was equal to or lower than that seen in the crystal structures, and the residues farther from the redox coordinating cysteines showed considerably less deviation in the minimized than in the crystal structures. Moreover, the largest RMSD per residue between the crystal structures of Pf is quite small, less than 0.5 Å (Fig. 3). Most importantly, the residues that make the largest contribution to the electrostatic reduction energy are those close to the coordinating residues for the redox site, and the shifts mentioned above at both coordinating loops are seen in the crystal structure.

Side-chain position changes in the minimized structure upon reduction were small. The large distance from the polar and charged side chains to the redox site and the diffuse charge distribution of the redox site result in small forces acting on the atoms, and there was little relaxation in portions of the protein far from the redox site. The RMSDs per residue for side-chain atoms alone between the OXD

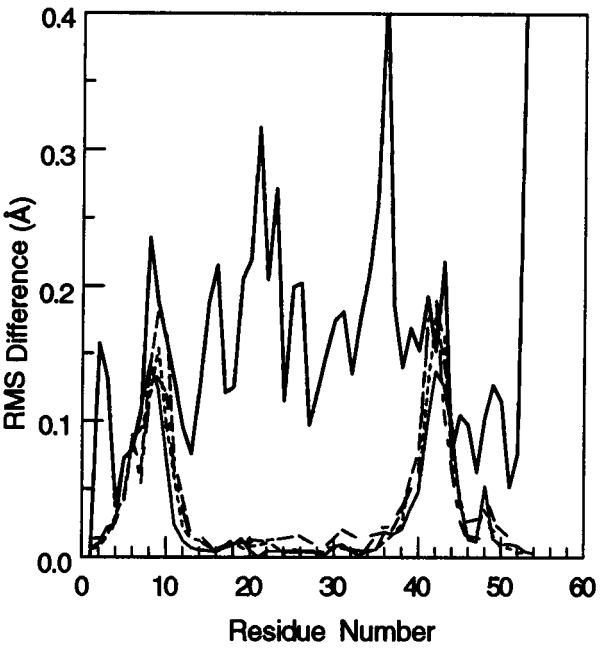

FIGURE 3 Root mean square differences in atomic position between the energy-minimized oxidized and reduced structures averaged over the backbone atoms N, Cα, and C for each residue in rubredoxin from *C. pasteurianum* (*dotted line*), *D. gigas* (*long and short dashed line*), *D. vulgaris* (*dashed line*), *P. furiosus* (*light solid line*), and the oxidized and reduced crystal structures for *P. furiosus* (Day et al., 1992) (*dark solid line*). Cysteines ligating the iron are at residues 6, 9, 39, and 42.

TABLE 1 Root mean square deviations in backbone atom positions between the oxidized crystal structures (XOXD) and the energy-minimized oxidized (OXD) and reduced (RED′) structures for *C. pasteurianum* (Cp), *D. vulgaris* (Dv), *P. furiosus* (Pf), and *D. gigas* (Dg) rubredoxins and for the crystal structures of the oxidized and reduced forms of the *P. furiosus* (Pfx) rubredoxins

	Dg	Dv	Pf	Cp	Pfx
XOXD-OXD	0.85	0.60	0.71	0.86	—
OXD-RED′	0.07	0.08	0.06	0.08	0.24

The oxidized and reduced crystal structures in Pfx are considered to represent the OXD and RED′ structures from the energy minimization studies. Values are given in Å.

and RED′ structures indicate again that very little structural relaxation occurs (0.29 Å maximum RMSD per residue), and again, the residues close to the redox site relax the most (Fig. 4). Side-chain relaxation in all of the rubredoxins was very similar and, in general, was a response to the backbone relaxation, because they were seen in the same residues and were of the same magnitude (Fig. 4).

The RMSD for side chains between the oxidized and reduced structures from crystal for Pf rubredoxin generally showed more movement than did the minimized redox pair. Moreover, in the reduced crystal structure of Pf, all of the charged side chains showed considerable movement toward or away from the redox site, depending on the charge of the side chain, with two lysines exhibiting dihedral transitions, none of which were observed in the energy minimization studies.

Protein reduction energy

The total energies were calculated for the OXD, RED*, and RED′ structures (Table 2). The energies for RED* are calculated using the oxidized structure, but with reduced charges and internal coordinate parameters for the redox site (see Methods); in addition, the energies are given for RED**, which is the oxidized structure but with reduced charges only. The energy differences between RED** and RED* are minimal. Energies are shown both with and without charged side chains (Table 2). Unless otherwise stated, the reduction energies due to the polar groups alone (Table 3) will be discussed, although the entire reduction energy of the redox system includes that of solvent and charged side chains. Here the reduction reaction of rubredoxin is divided into two events. The first is a Frank-Condon-type reduction of the redox site, which consists of an instantaneous change in the overall charge of the redox site from $-1e$ to $-2e$, where e is the charge of an electron, without allowing the protein to respond. The energy of the Frank-Condon reaction, referred to as ΔQ, ranged from -400 to -1200 mV. Cp had the highest ΔQ, which is primarily due to the amide group of Cys^9 being ~0.2 Å farther from the redox site than in the other three rubredoxins. The second event is the response of the protein to the change in charge of the redox site. The energy of this response, referred to as the relaxation energy, ranged from

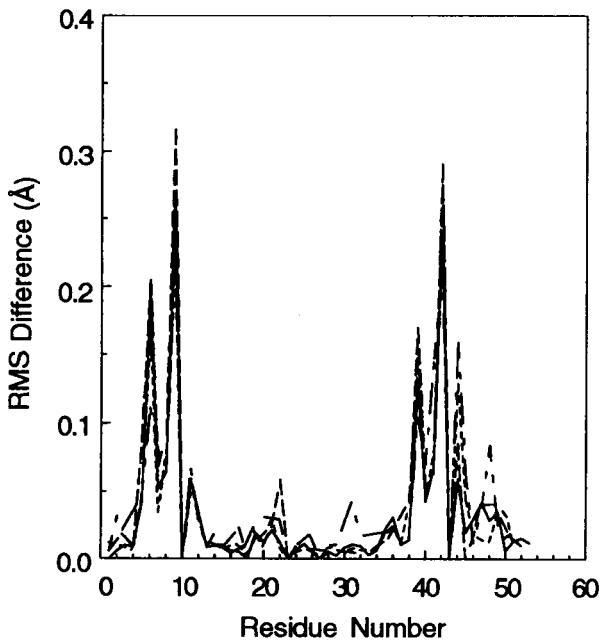

FIGURE 4 Root mean square differences in atomic position between the energy-minimized oxidized and reduced structures averaged over the side-chain atoms for each residue in rubredoxin from *C. pasteurianum* (*dotted line*), *D. gigas* (*long and short dashed line*), *D. vulgaris* (*dashed line*), and *P. furiosus* (*solid line*).

TABLE 2 Total energies for various structures calculated for the oxidized structures with oxidized energy parameters (OXD), the oxidized structures with reduced charge but oxidized internal coordinate parameters (RED), the oxidized structures with reduced energy parameters (RED*), and the reduced structures with reduced energy parameters (RED′)**

	Dg	Dv	Pf	Cp
With charged side chains				
OXD	−1679	−1740	−1888	−895
RED**	−1528	−1597	−1748	−624
RED*	−1523	−1593	−1744	−621
RED′	−1538	−1609	−1757	−647
Without charged side chains				
OXD	−1949	−1869	−1948	−1981
RED**	−1979	−1900	−1977	−1992
RED*	−1974	−1897	−1972	−1989
RED′	−1988	−1909	−1984	−2007

Values are given in kcal/mol.

TABLE 3 Changes in energy (in mV) of the protein due to change in redox state (ΔQ), protein relaxation (Relaxation), protein reduction (Reduction), and protein reduction relative to that of *P. furiosus* (Relative) for polar groups alone from this study for *C. pasteurianum* (Cp), *D. vulgaris* (Dv), *P. furiosus* (Pf), and *D. gigas* (Dg) rubredoxins and the crystal structures of the oxidized and reduced forms of the *P. furiosus* (Pfx) rubredoxins

	Dg	Dv	Pf	Cp	Pfx
ΔQ	−1104	−1202	−1060	−374	−1143
Relaxation	−600	−524	−493	−781	−508
Reduction	−1704	−1726	−1554	−1155	−1651
Relative to Pf (polar)	−150	−172	0	399	−97
Potential at Fe*	2610	2550	2670	2350	—
Exp. redox potential	6[#]	0[§]	0[¶]	−57[‖]	0[¶]
Net protein charge	−8	−7	−9	−13	−9

Also shown are changes in potential at the Fe (in meV) due to change in redox state (potential) from Swartz et al. (1996), experimental redox potentials, and net protein charge (in units of electron charge).

*Swartz et al. (1996).

[#]Moura et al. (1979).

[§]LeGall et al. (1988).

[¶]Adams (1992).

[‖]Lovenberg and Sobel (1965).

−500 to −800 mV. Cp had the most negative relaxation energy, again because of the backbone structure at Cys^9.

The total reduction energies due to polar groups alone ranged from −1200 to −1700 mV and can be compared to the experimental redox potentials (Table 3), because the redox potential differences are proportional to the negative of the energy differences (Eq. 1). However, to compare with experiment, relative energies must be considered, because the contribution of intrinsic electron affinity energy for the redox site is not known. The reduction energies relative to Pf showed that the predicted redox potentials for Cp were much more negative than the other three, as is true in the experiment, but the difference was overestimated.

DISCUSSION

The energy minimization methods used in this study do not perturb the structures significantly from the crystal structures. Earlier studies show that including crystal waters in a minimization of Cp rubredoxin significantly improves the structure compared to the vacuum energy minimization (Shenoy and Ichiye, 1993). Here, because the different crystal structures contained different amounts of water, a ~5-Å shell of water was added. This approach does not represent the structure of liquid water at room temperature and may tend to dampen the relaxation of the protein. However, this approach does prevent the large distortions seen in extensive minimizations of a protein in vacuum (Shenoy and Ichiye, 1993; Ichiye et al., 1986). In addition, the relaxation step used a constrained minimization procedure (see Methods). A previous study (Shenoy and Ichiye, 1993) has shown that unconstrained minimization results in dramatic changes in the protein structure, whereas constrained minimization results in much smaller perturbations; thus the constrained minimization also improves the results.

The calculations presented here show that, in rubredoxins, the protein reduction energy differences due to the polar groups of the protein correlate well with the experimental redox potential differences. This agrees with conclusions of previous work (Churg and Warshel, 1986; Churg et al., 1983; Swartz et al., 1996; Warwicker, 1995) that the electrostatic contributions of surface charged side chains (all side chains in the rubredoxin are at the surface) must be dampened and that the polar groups are the important determinant. The charged side-chain contributions are dampened by dielectric screening of the charges by the solvent, as has been shown in molecular dynamics estimates of the solvent relaxation energies (without counterions) around the oxidized minimized structures of this study (Swartz, 1996) and around crystal structures (Swartz et al., 1996). Furthermore, molecular dynamics simulations of Cp rubredoxin that include counterions along with solvent have shown that the two together almost exactly cancel the charged side-chain contributions (Yelle et al., 1995). These findings are also consistent with the experimental findings discussed in the Introduction. Thus we concentrate only on the polar contributions to the energies, as was done previously (Swartz et al., 1996).

The availability of crystal structures of both oxidation states of Pf rubredoxin (Day et al., 1992) provides an opportunity to evaluate our minimization procedure. The localized nature of the protein relaxation in our minimized Pf structures compared to the oxidized and reduced crystals structures of Pf (Fig. 3) requires some discussion. The crystal structures of the oxidized and reduced forms of Pf rubredoxin suggest that considerably more structural relaxation occurs in the protein backbone (Fig. 3) and that charged side chains exhibit more pronounced movement upon reduction than predicted by the minimization studies (Fig. 4). Overall smaller differences are not unexpected, because the energy minimization procedure was chosen specifically so that structural changes upon relaxation would be small. However, for Pf, the relaxation energies of the polar groups, as well as ΔQ energies, calculated from the oxidized and reduced crystal structures are quite similar to those calculated from the energy-minimized structures (Table 3). This is because the majority of the differences in structural relaxation between the crystal structures and the energy-minimized structures occur in regions that are far from the redox site, and because the regions close to the redox site not only contribute the most to the change in energy, but are the most similar in terms of the changes between the crystal structures and the minimized structures (Fig. 3). The physical interpretations of these results are based on the fact that charge-dipole interactions are relatively short range (i.e., as compared to charge-charge interactions). Thus the structural relaxation at long range is not seen here, because small barriers to the relaxation cannot be overcome simply by considering the charge-dipole interactions. These small barriers would be crossed in the real system because of thermal fluctuations. However, because the charge-dipole interactions are relatively short range, the contributions of the relaxation at long range is relatively small and thus will not contribute significantly to the differences in redox potential. On the other hand, the minimization procedure does appear to accurately predict the changes near the redox site, which also contribute the most. We also note that a more vigorous minimization procedure (i.e., one without constraints) may predict structural changes at longer range; however, for comparisons of different structures, it may be unreliable to use them, because different subsets of the long-range changes for different structures may be predicted as a result of slightly different barrier heights.

Overall, similarities between experiment and calculation in relaxation energy rather than in RMS differences per residue are more important. This is because RMS differences between the oxidized and reduced structures are based on a least-squares fit of the entire backbone; thus, even if the structural changes in the crystal and in minimized structures were identical, they would not necessarily appear to be the same. Superimposing limited regions of the protein only helps in part because the redox site also distorts slightly. In

fact, it is changes in the distances between the atoms of the redox site and those of the rest of the protein that are important. Furthermore, the importance of these changes is weighted by the energies. Thus the energy differences are the best measure. Hence, at least in the portion of the protein close to the redox site, the energy minimization study represents the structural relaxation of the protein relatively well.

Note that the results for the reduction energies of just the polar contributions show the same trends as the experimental redox potentials (Table 3), keeping in mind that the energy is proportional to the negative of the redox potential (Eq. 1). As pointed out by Swartz et al. (1996), rubredoxins of known sequence and redox potential can be separated into two groups separated by ~50 mV. Cp falls in a group of four rubredoxins that have redox potentials of about −50 mV and a Val at residue 44, whereas Dv, Dg, and Pf fall into a group of five rubredoxins that have redox potentials of ~0 mV and an Ala at residue 44. This sequence difference leads to a shift in the backbone of ~0.4 Å very near the redox site, and thus to a change in the polar contributions, which appears to be the root of the 50-mV difference (Swartz et al., 1996). The reduction energies, normalized to Pf (Table 3), indicate a clear difference between Cp and the higher potential rubredoxins in that the reduction energy of Cp was ~500 mV less negative. Although this is an overestimation of the difference, the overestimation would be even greater if relaxation were not included, because the relaxation energy of Cp is much greater than the other three. There is no obvious difference in the relaxation of Cp compared to the other three rubredoxins that can explain the larger relaxation energy, but the large difference in ΔQ between Cp and the other three was primarily due to the 0.2-Å shift of the amide group of Cys^9 away from the redox site.

Although the studies here predict the correct trend, they overestimate the experimental redox potential differences between Cp and the other three, which may come from a few sources. Residual energetic contributions of charged side chains, counterions, and solvent relaxation may cause slight differences, but, as mentioned above, the overwhelming experimental and computational evidence is that this should contribute a negligible amount. In addition, the structural contributions of charged side chains and solvent were included in the energy minimization steps, although not in the final energies in Table 3, and the good agreement between the minimized and crystal structures for oxidized and reduced Pf in Table 3 and Fig. 3 indicate that the energy minimization adequately describes both oxidized and reduced structures. Another important factor is electronic polarization; however, the CHARMM and TIP3P potentials include electronic polarization implicitly via the partial charges. The doubly charged reduced redox site will induce slightly more electronic polarization; however, studies of ions in water indicate that electronic polarization becomes important only for charges greater in magnitude than $2e$ (David Smith, personal communication), and in addition, the change here is quite diffuse, because it is spread over the entire redox site. A third factor to consider is the partial charges of the redox site; however, other studies (Churg et al., 1983; Shenoy and Ichiye, 1993; Jensen et al., 1994) indicate that the results are relatively insensitive to the exact charge distribution used. As a whole, the overestimation is probably due to the exaggerated shift of Cys^9 in Cp rubredoxin during the initial minimization of the oxidized form, which is caused by inaccuracies in the interaction potential.

The results presented here can also be compared to our earlier calculations. This work is a considerable improvement over our previous minimization study of Cp rubredoxin alone (Shenoy and Ichiye, 1993), because the RMS differences of the OXD structure from the crystal structure here are 0.30 Å less than previously reported, because of the additional water beyond crystal water (see Methods), indicating that the structures here are probably better. Furthermore, Shenoy and Ichiye (1993) indicate that there was a constriction of the redox site that may be indicative of a general constriction of the protein, which did not occur to as great an extent here, giving rise to a lower RMS difference with the crystal and lower ΔQ in the present studies. Most important, the relaxation energy here is very close to the previous result of ~16 kcal/mol, although the RMS difference between the OXD and RED′ structures is 0.06 Å less than that reported by Shenoy and Ichiye (1993).

This work also presents an interesting contrast to a previous study of the same proteins, in which crystal structures were used (Swartz et al., 1996) instead of the energy-minimized structures used here. Because there is no structural relaxation in the charge change step of the reduction reaction, the energy due to charge change of the redox site, ΔQ, is similar in definition to the negative of the electrostatic potential calculations in Swartz et al. (1996) (Table 3). However, the values are different, partly because of the differences between the energy-minimized versus crystal structures. More important is the fact that here the difference in the interaction energy between the redox site (via the partial charges) and the rest of the protein is reported, whereas in Swartz et al. (1996) the electrostatic potential at the iron is reported. If the change in charge of the redox site were concentrated at the Fe rather than being distributed over the Fe, S, and C, the calculations would be the same. Because this is not the case, here the potential changes at all of the atoms of the FeS site are probed. Moreover, because of the exclusion rules for bonded atoms in the nonbonded interactions, the contributions of the cysteinyl backbone groups will be severely modified. However, this contribution appears to make mainly an additive difference. Thus the differences in ΔQ between Cp and the other three here can be compared with the differences in potential in Swartz et al. (1996). The remarkably good results in Swartz et al. (1996) were obtained because the important contributions to the electrostatics come from polar groups and because the structure of the polar groups was accurately represented in the high-resolution crystal structures used in those calculations. Here again, the focus on the polar groups leads to good results, although the exaggerated shift of Cys^9 in Cp

causes the difference in ΔQ of Cp from the other three to be too large. More generally, it appears that energy minimization may cause unequal distortion of the structures, so that using crystal structures may be more accurate for determining the ΔQ contribution. However, to obtain the relaxation energy, energy minimization must be used. Thus the fact that the correct trends in ΔQ were obtained with the energy-minimized structures is important (even if the results were not as good as those obtained from crystal structures). Moreover, it indicates that the changes in structure and thus in energy upon change in redox state are reasonable, because the starting structures are reasonable. The constrained minimization ensured reasonable relaxation.

In sum, our earlier study of the energetics of the crystal structures of the same homologous rubredoxins (Swartz et al., 1996) may be the most reliable means of determining the ΔQ contribution at this time. Our studies indicated that the unconstrained minimization here and molecular dynamics (Yelle et al., 1995) cause a large enough deviation to be less accurate than the crystal structure. However, the accuracy is sufficient to reproduce general trends. Constrained minimization may be a better compromise. On the other hand, the relaxation contribution can only be determined through computational methods such as energy minimization or molecular dynamics, unless crystal or NMR structures are available for both forms.

CONCLUSIONS

Previously reported experimental results suggest that the structural differences in the redox site and charged side-chain distribution of iron-sulfur redox proteins cannot account for their differences in redox potential. The remaining protein component that can influence the redox potential is then polar groups, of which only those close to the redox site will influence the potential. By comparison with oxidized and reduced crystal structures of Pf rubredoxin, the constrained energy minimization methods used here are shown to represent well the crucial protein backbone and polar side-chain structural relaxation near the redox site, although not the relaxation of portions of the protein farther from the redox site. However, the latter does not contribute significantly to the electrostatic potential at the redox site, and so the relaxation energies from energy minimization agree well with those from crystal structures. In addition, as in Swartz et al. (1996), the energy contribution without relaxation predicts that Cp has a lower redox potential than Dv, Dg, and Pf. The relaxation energy of backbone polar groups in Cp is ~250 mV greater than the other three rubredoxins studied here, and this relaxation energy is necessary to bring the magnitude of the energy difference between Cp and the other three into better agreement with experimental values. Overall, the relaxation energy is shown to be large (500–800 mV), by both the energy minimizations and the crystal results, and considerable variations in the relaxation energy (a range of 300 mV) due to polar groups near the redox site are possible, even with very similar structure near the redox site. Thus the relaxation energy is an important factor to consider in the energetics of reduction.

The authors thank Dr. Douglas Rees for providing coordinates for *Pyrococcus furiosus* rubredoxin. We also thank the Visualization, Analysis and Design in the Molecular Sciences (VADMS) Laboratory at Washington State University and Dr. Gerald Hazelbauer for providing additional computational resources.

This work was supported by a grant from the National Institutes of Health (1 R29 GM45303).

REFERENCES

Adams, M. W. W. 1992. Novel iron-sulfur centers in metalloenzymes and redox proteins from extremely thermophilic bacteria. *Adv. Inorg. Chem.* 38:341–396.

Adman, E., L. C. Sieker, and L. H. Jensen. 1991. Structure of rubredoxin from *Desulfovibrio vulgaris* at 1.5 Å resolution. *J. Mol. Biol.* 217: 337–352.

Allen, M. P., and D. J. Tildesley. 1987. Computer Simulations of Liquids. Oxford University Press, Oxford.

Backes, G., Y. Mino, T. M. Loehr, T. E. Meyer, M. A. Cusanovich, W. V. Sweeney, E. T. Adman, and J. Sanders-Loehr. 1991. The environment and Fe_4S_4 clusters in ferredoxins and high-potential iron proteins. New information from x-ray crystallography and resonance Raman spectroscopy. *J. Am. Chem. Soc.* 113:2055–2064.

Brooks, B. R., R. E. Bruccoleri, B. D. Olafson, D. J. States, S. Swaminathan, and M. Karplus. 1983. CHARMM: a program for macromolecular energy, minimization, and dynamics calculations. *J. Comput. Chem.* 4:187–217.

Bruccoleri, R. E., and M. Karplus. 1986. Spatially constrained minimization of macromolecules. *J. Comput. Chem.* 7:165–175.

Churg, A. K., and A. Warshel. 1986. Control of the redox potential of cytochrome *c* and microscopic dielectric effects in proteins. *Biochemistry.* 25:1675–1681.

Churg, A. K., R. M. Weiss, A. Warshel, and T. Takano. 1983. On the action of cytochrome *c*: correlating geometry changes upon oxidation with activation energies of electron transfer. *J. Phys. Chem.* 87: 1683–1694.

Day, M. W., B. T. Hsu, L. Joshua-Tor, J.-B. Park, Z. H. Zhou, M. W. W. Adams, and D. C. Rees. 1992. X-ray crystal structures of the oxidized and reduced forms of the rubredoxin from the marine hyperthermophilic archaebacterium *Pyrococcus furiosus*. *Protein Sci.* 1:1494–1507.

Frey, M., L. Sieker, F. Payan, R. Haser, M. Bruschi, G. Pepe, and J. LeGall. 1987. Rubredoxin from *Desulfovibrio gigas*: a molecular model of the oxidized form at 1.4 Å resolution. *J. Mol. Biol.* 197:525–541.

Gane, P. J., R. B. Freedman, and J. Warwicker. 1995. A molecular model for the redox potential difference between thioredoxin and DsbA, based on electrostatics calculations. *J. Mol. Biol.* 249:376–387.

Gleason, F. K. 1992. Mutation of conserved residues in *Escherichia coli* thioredoxin: effects on stability and function. *Protein Sci.* 1:609–616.

Hugenholtz, J., and L. G. Ljungdahl. 1990. Metabolism and energy generation in homoacetogenic clostridia. *FEMS Microbiol. Rev.* 87: 383–390.

Ichiye, T., B. D. Olafson, S. Swaminathan, and M. Karplus. 1986. Structure and internal mobility: a molecular dynamics study of hen egg-white lysozyme. *Biopolymers.* 25:1909–1937.

Jensen, G. M., A. Warshel, and P. J. Stephens. 1994. Calculation of the redox potentials of iron-sulfur proteins: the 2−/3− couple of $[Fe_4S^*4Cys_4]$ clusters in *Peptococcus aerogenes* ferredoxin, *Azotobacter vinelandii* ferredoxin I, and *Chromatium vinosum* high-potential iron protein. *Biochemistry.* 33:10911–10924.

Jorgensen, W. L. 1981. Transferable intermolecular potential functions for water, alcohols and ethers. Application to liquid water. *J. Am. Chem. Soc.* 103:335, 341, 345.

Langen, R., G. D. Brayer, A. M. Berghuis, G. McLendon, F. Sherman, and A. Warshel. 1992a. Effect of the Asn52-Ile mutation on the redox potential of yeast cytochrome *c*. Theory and experiment. *J. Mol. Biol.* 224:589–600.

Langen, R., G. M. Jensen, U. Jacob, P. J. Stephens, and A. Warshel. 1992b. Protein control of iron-sulfur cluster redox potentials. *J. Biol. Chem.* 267:25625–25627.

LeGall, J., B. C. Prickril, I. Moura, A. V. Xavier, J. J. Moura, and B. H. Huynh. 1988. Isolation and characterization of rubrethyrin, a non-heme iron protein from *Desulfovibrio vulgaris* that contains rubredoxin centers and hemerythrin-binuclear iron cluster. *Biochemistry.* 27:1636–1642.

Liu, Y., and T. Ichiye. 1994. An integral equation theory for the structure of water around globular solutes. *Chem. Phys. Lett.* 231:380–386.

Lovenberg, W., and B. Sobel. 1965. Rubredoxin: a new electron transfer protein from *Clostridium pasteurianum. Proc. Natl. Acad. Sci. USA.* 54:193–199.

Moura, I., J. J. G. Moura, M. H. Santos, A. V. Xavier, and J. LeGall. 1979. Redox studies on rubredoxins from sulphate and sulphur reducing bacteria. *FEBS Lett.* 107:419–421.

Rychaert, J. P., G. Cicotti, and H. J. C. Berendsen. 1977. Numerical integration of the Cartesian equation of motion of a system with constraints: molecular dynamics of *n*-alkanes. *J. Comput. Chem.* 23: 327–341.

Seki, Y., S. Seki, M. Satch, A. Ikeda, and M. Ishimoto. 1989. Rubredoxin from *Clostridium perfringens*: complete amino acid sequence and participation in nitrate reduction. *J. Biochem. (Tokyo).* 106:336–341.

Shen, B., D. R. Jolles, D. C. Stout, T. C. Diller, F. A. Armstrong, C. M. Gorst, G. N. La Mar, P. J. Stephens, and B. K. Burgess. 1994. *Azotobacter vinelandii* ferredoxin I. *J. Biol. Chem.* 269:8564–8575.

Shenoy, V. S. 1992. Contribution of protein environment to redox potentials of rubredoxin and cytochrome *c*. MS thesis. Washington State University, Pullman, WA.

Shenoy, V. S., and T. Ichiye. 1993. Influence of protein flexibility on the redox potential of rubredoxin: energy minimization studies. *Protein Struct. Funct. Genet.* 17:152–160.

Sieker, L. C., R. E. Stenkamp, L. H. Jensen, B. C. Prickril, and J. LeGall. 1986. Structure of rubredoxin from the bacterium *Desulfovibrio desulfuricans. FEBS Lett.* 208:73–76.

Steinbach, P. J., and B. R. Brooks. 1994. New spherical-cutoff methods for long-range forces in macromolecular simulation. *J. Comput. Chem.* 15:667–683.

Stenkamp, R. E., L. C. Sieker, and L. H. Jensen. 1990. The structure of rubredoxin from *Desulfovibrio desulfuricans* strain 27774 at 1.5 Å resolution. *Proteins Struct. Funct. Genet.* 8:352–364.

Swartz, P. D. 1996. Computational models of redox proteins and protein model building. Ph.D. thesis. Washington State University, Pullman, WA.

Swartz, P. D., B. W. Beck, and T. Ichiye. 1996. Structural origins of redox potentials in Fe-S proteins: electrostatic potentials of crystal structures. *Biophys. J.* 71:2958–2969.

Sweeney, W. V., and J. C. Rabinowitz. 1980. Proteins containing 4Fe-4S clusters: an overview. *Annu. Rev. Biochem.* 49:139–161.

Warwicker, J. 1994. Improved continuum electrostatic modelling in proteins, with comparison to experiment. *J. Mol. Biol.* 236:887–903.

Watenpaugh, K., L. C. Sieker, and L. H. Jensen. 1980. Crystallographic refinement of rubredoxin at 1.2 Å resolution. *J. Mol. Biol.* 138:615–633.

Yelle, R. B., N.-S. Park, and T. Ichiye. 1995. Molecular dynamics simulations of rubredoxin from *Clostridium pasteurianum*: changes in structure and electrostatic potential during redox reactions. *Proteins.* 22:154–167.

Zeng, Q., E. T. Smith, D. M. Kurtz, and R. A. Scott. 1996. Protein determinants of metal site reduction potentials. Site-directed mutagenesis studies of *Clostridium pasteurianum* rubredoxin. *Inorg. Chim. Acta.* 242:245–251.